



## Influence of carbon carriers on catalytic performance of Ni/C catalysts for vapor-phase carbonylation of ethanol

Jun Song<sup>1</sup>, Li Wang<sup>2</sup>, Gang Song<sup>3</sup> and Jian Wang<sup>1</sup>

<sup>1</sup>Chemistry and Chemical Engineering School, Northeast Petroleum University, Daqing, China

<sup>2</sup>Petrochina Qaqing Refining & Petrochemical Company, Daqing, China

<sup>3</sup>Communication Training Base of General Staff, Zhangjiakou, China

### ABSTRACT

Different active carbons were used to prepare Ni based catalysts for vapor-phase carbonylation of ethanol. N<sub>2</sub> physical adsorption, X-ray photoelectron spectroscopy, infrared spectrometry and Scanning electron microscopy were used to investigate the structural properties of carbon carriers. The activity of Ni/C supported catalyst were also studied. The results revealed that wood charcoal had a considerable number of mesopores, higher specific surface area and more oxygen-containing groups which contained C=O functional group on the surface. Ni/C catalyst prepared by wood charcoal showed the highest catalytic activity for ethanol carbonylation with 67.62% of ethanol conversion and 65.48% of product combined selectivity.

**Keywords:** carbon carrier; ethanol; vapor-phase carbonylation

### INTRODUCTION

Studies showed that [1-3], catalysts which was prepared using activated carbon as carrier, showed good performance in the process of the carbonylation of ethanol. In this paper, 4 kinds of active carbon were selected as carrier which catalysts were prepared with. The effects of carbon material such as physical properties, chemical composition and surface texture of activated carbon on dispersion state of Ni and catalytic performance of nickel catalyst were further investigated. Combined with the study on supported catalyst properties, a significant reference was provided for screening out the ideal carbon carrier.

### EXPERIMENTAL SECTION

#### Carbon carriers and pretreatment

Activated carbon carriers chosen in the experiment were as follow: C1, wood charcoal; C2, shell charcoal; C3 coconut shell charcoal; C4 bamboo charcoal. Before experiment, the above activated carbons were ground, then passed through 20-30 mesh sieve, and dried for 4 hours in an oven at 120 °C.

#### Characterization of carbon carriers

N<sub>2</sub> physical adsorption of activated carbon was carried out at the NOVA 2000e surface area & pore size analyzer of American Quantachrome Instruments. BET equation are used to calculate the sample's specific surface area, and the pore size distribution was calculated by BJH method.

Activated carbon crystal phase analyzed by D/Max-2200 X-ray diffractometer of Japan co., LTD. Test conditions: Cu target, K $\alpha$  characteristic diffraction radiation, graphite monochromatic filter, slit SS/DS1°, RS 0.15 mm, working voltage was 40 kV, current was 100 mA, SC counter, scanning speed was 40°/min, the speed of stepper was 0.02°, scanning range was 10°-80°.

The identification and structural analysis of activated carbon's organic functional group was tested on TENSOR27 Fourier transform infrared spectrometer. When testing, a moderate amount of samples were mixed with KBr powder, and the mixture were ground fully, then tableted, the detection range was 400-4000  $\text{cm}^{-1}$ .

Carriers and catalysts surface microscopic/ submicroscopic morphology were observed via CBI 3JS field emission scanning electron microscope.

#### Preparation and performance evaluation of supported catalyst

With 4 kinds of activated carbon as carriers, nickel acetate for the precursor, Ni/C catalysts were prepared by equivalent-volume impregnation. The catalysts were stirred continuously for 12 hours during immersion, then dried for 3 hours in an oil bath at 60-70 with stirring continuously, then placed in a dryer, heated slowly up to 120, dried isothermally for 12 hours.

The active evaluation of catalyst was carried out in a fix-bed continuously flowing micro-type reactor. The reaction tube was made of quartz glass, the diameter of the tube was 12mm and length 350mm, the loading quantity of the catalyst was 2g. Before reacted, catalysts were calcined for 2 hours under  $\text{N}_2$  atmosphere, then reduced for 2 hours under  $\text{H}_2$  atmosphere. After the temperature of catalysts fell to the reaction temperature, liquid raw materials ethanol and iodine ethane were pumped into the reaction system by a double-plunger pump, mixed fully with CO after gasification, then blend into reactor. The products were condensed and analyzed by the gas chromatograph with hydrogen flame detector. Reaction conditions:  $n(\text{CO}) : n(\text{EtOH}) : n(\text{EtI}) = 20 : 10 : 1$ , detecting temperature was 260, atmospheric pressure. Catalytic activity was evaluated by parameters selected including the conversion of ethanol in the raw materials, the combined selectivity of product propionic acid and ethyl propionate.

## RESULTS AND DISCUSSION

#### The specific surface area and pore structure parameters of activated carbon as carrier

At liquid nitrogen temperature  $-196^\circ\text{C}$ , the 4 kinds of activated carbon physically adsorbed adsorbate nitrogen, adsorption-desorption isotherms were obtained in Figure 1 according to the experimental data.

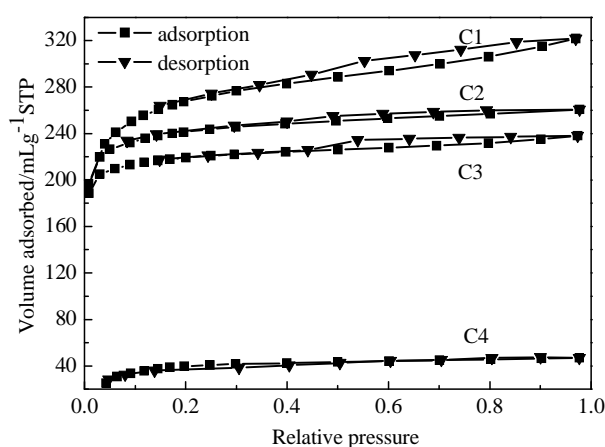


Fig.1 Nitrogen adsorption-desorption isotherms of the active carbons

It can be seen from figure 1, according to the BDDT (Brunauer-Deming-Deming-Teller) classification, all the isotherms of activated carbon belonged to type II except the bamboo charcoal. The isotherm of bamboo charcoal belonged to type I, no obvious hysteresis loop was observed,  $\text{N}_2$  adsorption capacity increased dramatically from the origin at low pressure area, while increased slowly in the high pressure area. The  $\text{N}_2$  adsorption quantity was small, which indicated that there were no mesoporous in the carbon and it's a typical microporous material. Adsorption curve of shell charcoal was relatively flat in the high pressure area, the hysteresis loop was slightly larger, and the adsorption amount of  $\text{N}_2$  was increased, all indicated that the pores in shell charcoal was mainly microporous and there were also a small amount of the mesoporous. Adsorption isotherms of wood charcoal and coconut shell carbon had obvious hysteresis loop, the  $\text{N}_2$  adsorption amount of wood charcoal was the maximum, indicating that it had a large quantity of mesoporous structure and some macroporous, while the coconut shell charcoal had adequate mesoporous and few macroporous.

Specific surface area and pore structure parameter of activated carbons calculated by physical adsorption data were showed in table 1. we can see from table 1 that the specific surface area of activated carbons made of different

materials varied greatly. Specific surface area of the bamboo charcoal was the smallest 132.99 m<sup>2</sup>/g, followed by the coconut charcoal, that of wood charcoal and shell charcoal was larger than the above, especially specific surface area of wood charcoal 831.79 m<sup>2</sup>/g was the largest. Total pore volumes of carbon materials showed the same rules with the specific surface area, wood charcoal C1 had the maximum total pore volume, which indicated that there were plentiful pore structures in it; bamboo charcoal had the minimum total pore volume, only 0.0724 mL/g.

**Tab.1 Surface area and pore structure parameters for different activated carbon**

Activated carbon	Surface area /m <sup>2</sup> /g	Pore volvm /mL/g	Average pore diameter /nm	Pore diameter distribution (%)		
				<2nm	2-50nm	>50nm
C1	831.79	0.4975	2.392	74.3	19.2	6.5
C2	736.12	0.4031	2.191	79.8	13	7.2
C3	665.32	0.3861	2.213	81.5	15.2	3.3
C4	132.99	0.0724	2.177	86.8	5.2	8

As a microporous material, the activated carbon had few pores which diameter was larger than 50nm. In bamboo charcoal pore structures, microporous which diameter was smaller than 2nm occupied the highest proportion, provided 80% of the total pore volume. Micropores also had a high proportion in shell charcoal, and some mesoporous in it additionally. In the wood carbon and coconut shell carbon, proportion of mesoporous was slightly higher, that of wood charcoal accounted for 19.2%, which was the largest proportion of all the activated carbon. The average pore diameter of activated carbon was about 2nm. Average pore diameter of C1 was the maximum, on account of its containing a certain amount of mesoporous, and bamboo charcoal had mainly microporous with the minimum average pore diameter.

#### The XRD spectra of carbon carrier

The XRD spectra of original activated carbons are showed in Fig. 2.

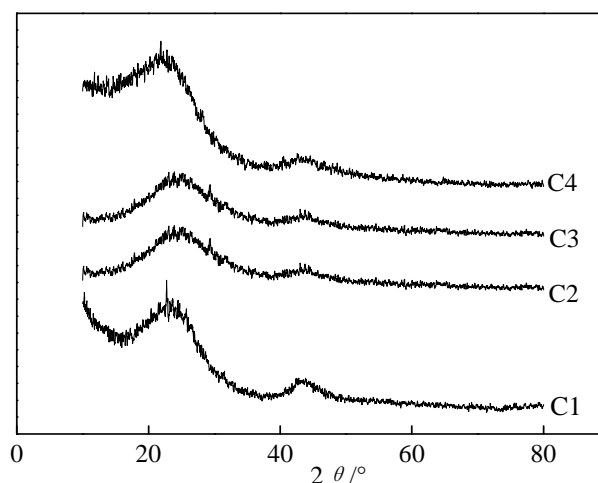


**Fig.2 XRD spectra of original carbons**

It can be seen from Fig. 2, 2θ had two distinct irregular peaks between 20-30°, 40-50° in the diffraction pattern of activated carbon. It corresponded to the broad diffraction peak of graphite structure (002), (100) crystal face. That's attributed to irregular arrangement of the tiny graphite crystal in the activated Carbon. Activated carbon was microcrystal carbon structure, in this diffraction spectra, characteristic spectral line of activated carbon became wider and the strength weaker which showed that the activated carbon was amorphous structure. The diffraction peaks of C1 and C4 were a bit stronger on the (002) crystal face, in general, the diffraction patterns of 4 kinds of activated carbon carrier materials was not much difference, indicating crystal structure of the original carbon materials were similar, and all belonged to the graphite crystal which were non-regular arrangement.

#### Infrared spectrum analysis of carbon carrier

In order to grasp the surface chemical properties of activated carbon, different carbon carriers have been characterized by using infrared spectrometry respectively. Infrared spectrograms of different carbon carriers were showed in Figure 3.

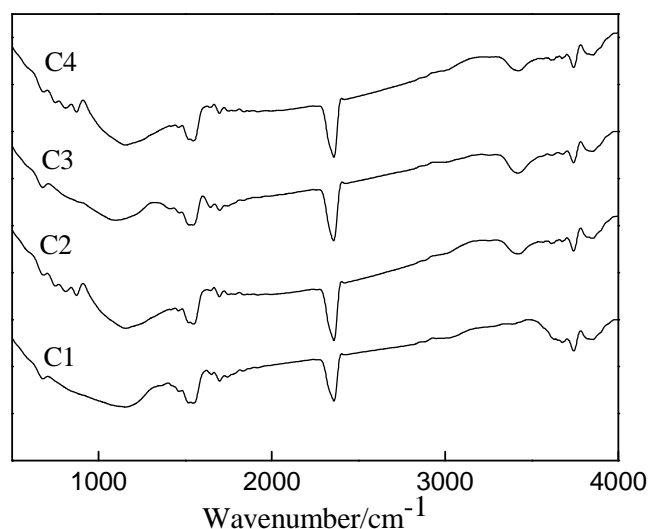


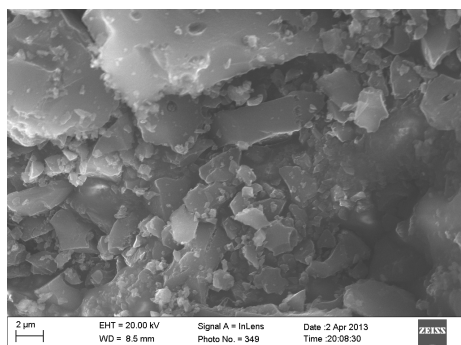
**Fig.3 FTIR spectra for activated carbon carriers**

The species and quantities of organic functional groups on carbon surface can be seen from Fig.3. Among them, there was obvious absorption peak around 3420  $\text{cm}^{-1}$ , belonging to the stretching vibration of sample surface of hydroxyl O-H key, it may be  $-\text{OH}$  in  $-\text{COOH}$  groups or the sample surface physical adsorption of water [4]; The absorption peak around 2400  $\text{cm}^{-1}$  belonged to  $\text{C}\equiv\text{N}$  and  $\text{C}\equiv\text{C}$  characteristic peak [5]. The Smaller absorption peak around 1600  $\text{cm}^{-1}$  belonged to stretching vibration[6] of skeleton  $\text{C}=\text{C}$  in aromatic hydrocarbons or  $-\text{OH}$  in  $-\text{COOH}$  groups;The absorption peak around 1580 $\text{cm}^{-1}$  belonged to  $\text{C}=\text{O}$  functional groups(carboxyl、 anhydride、 lactone etc.) [7-9]. Thus the activated carbon contained a certain amount of nitrogen-containing functional groups and reductive unsaturated functional groups  $\text{C}\equiv\text{N}$ ,  $\text{C}\equiv\text{C}$ , in addition, its surface also contained carboxyl, carbonyl group, lactone group, and many other types of oxygen-containing groups.The species and quantities of surface oxygen functional groups of different kinds of activated carbons were almost the same, among them stretching vibration of  $-\text{OH}$  in C1 was a bit weaker, while symmetric stretching vibration of oxygenic  $\text{C}-\text{O}-\text{C}$  around  $1000^{-1}$ -250 $\text{cm}^{-1}$  was stronger, which show that it contained more structures of the ether bond  $\text{C}-\text{O}-\text{C}$  and lactone structures and less hydroxyl structures.

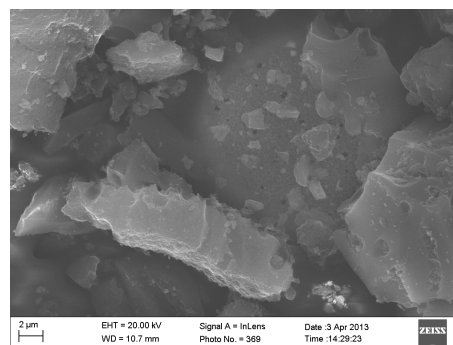
#### Scanning electron microscopy photos of carbon carrier

In order to observe the surface morphology of carbon carriers, the different activated carbons were observed under the scanning electron microscopy. Figure 4 was the photos of activated carbon surface magnified 10000 times.

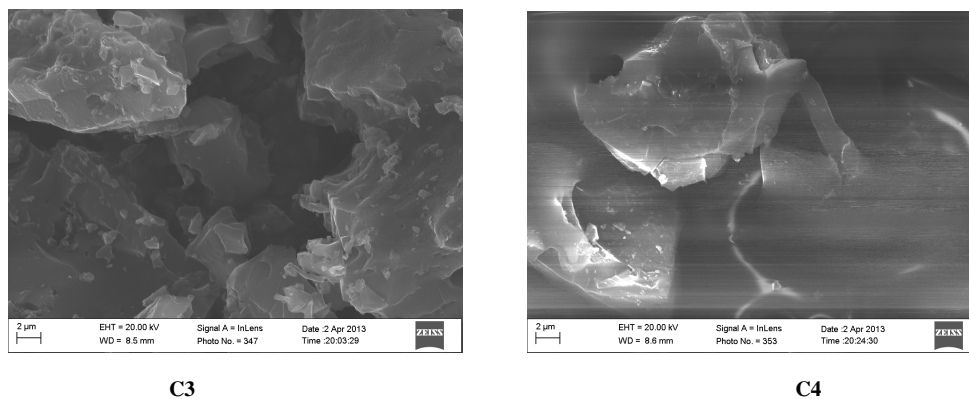
It can be seen from the figure 4, the surface morphology of different carbon carriers were quite different, flake particles on wood charcoal surface were more uniform and average particle size was smaller; particles on bamboo charcoal surface were larger, and the surface was smooth; particle size of fruit carbon and coconut charcoal were between the two.The active ingredient precursors dispersed easily and evenly on the wood charcoal which surface particles were uniform;Bamboo charcoal surface was smooth, particle size was large and uneven, the precursor of active components was difficult to disperse evenly on it, the force between precursor and arbon carrier was less, and the precursor were easy to volatilize and lost in subsequent processing steps which might cause the decrease of the number of active center and the decrease of the activity.



**C1**



**C2**



C3

C4

Fig.4 SEM images of activated carbons

### Catalyst activity of different carbon carriers

Catalyst activity of Ni/C catalysts supported on different active carbons in ethanol carbonylation reaction were studied, the results were shown in figure 5.

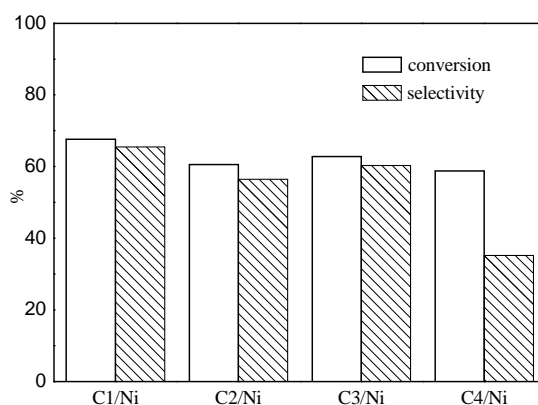


Fig.5 The activity of Ni/C catalysts supported on different active carbons

It can be seen from Figure 5, the activity of the C4/Ni catalyst was the lowest, ethanol conversion and propionic acid and ethyl propionate combined selection were 58.78% and 35.15%, respectively. The activity of C4/Ni catalyst prepared by wood charcoal carriers was the highest, the conversion of ethanol and selection of propionic acid were 67.62% and 65.48% respectively. The activity of the C2/Ni and C3/Ni catalyst prepared by fruit carbon and coconut charcoal carriers respectively were middle, and the activity of the C3/Ni catalyst was slightly higher than C2/Ni.

Catalyst preparation and evaluation were completed in the same experimental conditions. The activity differences of the 4 catalysts were caused by the differences of the carbon carrier structure. The specific surface area of wood activated carbons C1 was the maximum. Apart from being rich in micro-hole structure, it contained a certain amount of the available middle-pore structure and much oxygen functional groups on the surface, particularly the number of surface carboxyl groups was the largest. The nickel salt precursor of C1/Ni catalyst was dispersed and fixed in the inner surface of the carbon carrier easily due to all these physical and chemical properties, and then the precursor was activated and reduced to form active centers. So the catalytic activity of C1/Ni was the highest.

## CONCLUSION

Physical and surface chemical properties of activated carbon carrier materials were significantly different, which led to the differences of the performances of corresponding Ni/C catalyst for vapor-phase carbonylation of ethanol. Bamboo charcoal was a typical microporous material, with a strong adsorption capacity. The nickel precursor accumulated on the surface, which would not be benefit to the dispersion and reduction of the active components on its surface. In addition, the groups containing C=O functional group such as the lactone group, carboxylic acid anhydride or carbonyl group were less in the surface. Dispersion of Ni was poor in the Ni/BC catalyst, the ethanol conversion and propionic acid and ethyl propionate combined selection were both the lowest, 58.78% and 35.15% respectively. Physical and chemical performance parameters of fruit carbon and coconut charcoal ranged in the middle, so the dispersion situation of active ingredient on the surface had improved, and the

interaction between active ingredient and carriers weakened. That was conducive to the reduction of Ni component, which due to the increasing of the catalyst activity. Wood charcoal had a considerable number of mesopores, higher specific surface area and more oxygen-containing groups which contained C=O functional group such as lactone, carboxylic acid anhydride or carbonyl on the surface. In the catalyst Ni/C1 prepared by wood charcoal, the dispersion of Ni was the highest, the precursor was easily to reduce to active single substance Ni, meanwhile it was conducive to desorption of product molecules, and conversion of ethanol and combined selection of product both were the highest, 67.62% and 65.48% respectively.

#### REFERENCES

- [1] Kang Min, Lee Chang-Ha. *Carbon*, **2005**, 43(7): 1512-1516.
- [2] ML Toebes, JA Dillen, KP Jong. *Journal of Molecular Catalysis A*, **2001**, 173(1/2): 75-98.
- [3] AP Rajput and MK Patel, *Journal of Chemical and Pharmaceutical Research*, **2012**, 4(8): 3959-3965.
- [4] Park. S J, Jang Y S. *J. Colloid Interface Science*, **2002**, 249(02): 458-463.
- [5] Yang Hui-Zhu, Liu Zhi-Ying, Li Lei, et al. *Environment Pollution and Control*, **2009**, 31(10):10-14.
- [6] Burg P, Fydrych P, Cagniant D, et al. *Carbon*, **2002**, 40(09):1521-1531.
- [7] Zhang L, Chang X J, Li Z H, et al. *J. Molecular Structure*, **2010**, 964(1-3):58-62.
- [8] Zhu J Z, Deng B L, Yang J, et al. *Carbon*, **2009**, 47 (08):2014-2025.
- [9] Justin Masih, *Journal of Chemical and Pharmaceutical Research*, **2010**, 2(2): 546-553.